On the Climatic Impact of Ocean Circulation

MICHAEL WINTON

NOAA/Geophysical Fluid Dynamics Laboratory, Princeton, New Jersey

(Manuscript received 18 December 2002, in final form 18 March 2003)

ABSTRACT

Integrations of coupled climate models with mixed-layer and fixed-current ocean components are used to explore the climatic response to varying magnitudes of ocean circulation. Four mixed-layer ocean experiments without ocean heat transports are performed using two different atmosphere–land components—the new GFDL AM2 and the GFDL Manabe Climate Model (MCM)—and two different sea ice components, one dynamic and one thermodynamic. Both experiments employing the dynamic sea ice component develop unstable growth of sea ice while the experiments with a thermodynamic sea ice component develop very large but stable ice covers. The global cooling ranges from modest to extreme in the four experiments.

Using the fixed-current climate model, a trio of 100-yr integrations are made with control currents from a GFDL R30 ocean simulation, same currents reduced by 50%, and same currents increased by 50%. This suite is performed with two coupled models again employing the two atmosphere–land components, AM2 and MCM, for a total of six experiments. Both models show a large sensitivity of the sea ice extent to the magnitude of currents with increased currents reducing the extent and warming the high latitudes. Low cloud cover also responds to circulation changes in both models but in the opposite sense. In the AM2-based model, low cloudiness decreases as ocean circulation increases, reinforcing the sea ice changes in reducing the planetary reflectivity, and warming the climate. This cloudiness change is associated with a reduction in lower-atmospheric stability over the ocean. Because the AM2-based model is able to simulate the observed seasonal low cloud–stability relationship and the changes in these quantities with altered ocean circulation are consistent with this relationship, the AM2 interpretation of the cloud changes is favored.

1. Introduction

The oceans play two important thermal roles in climate: 1) they store and release heat seasonally, and 2) they move heat around in their large-scale current systems. This study is concerned with the second role. In addition to its obvious theoretical interest, the question has practical application to coupled climate model drift. An atmosphere model forced with observed SSTs will expect a horizontally varying net heat flux from the ocean. It will expect an annual mean flux of heat out of the Gulf Stream off the U.S. east coast, for example. If the ocean circulation of a coupled model provides a different net heat flux, the SSTs and sea ice distribution will drift away from observations. The drift will be large or small, local or global, depending upon how feedbacks in the climate system respond to the SST (and sea ice) changes, how they enhance or diminish them. The climate feedbacks that come into play when ocean circulation varies are the focus of this study.

We might expect to get some idea of the importance of oceanic heat transport (OHT) to climate by comparing it to atmospheric heat transport (AHT). Oceanic and atmospheric heat transports can be calculated from observations. The total heat transport is observed from satellites as the integrated net radiative flux at the top of the atmosphere: the absorbed shortwave minus outgoing longwave radiation (OLR). The atmospheric transport can be estimated from atmospheric observations and then subtracted from the total to give the ocean heat transport. Trenberth and Caron (2001) have used Earth Radiation Budget Experiment (ERBE) radiation data in conjunction with both the National Centers for Environmental Prediction (NCEP) and European Centre for Medium-Range Weather Forecasts (ECMWF) reanalyses to obtain transport estimates. The average of the two Trenberth and Caron estimates is shown in Fig. 1. Trenberth and Caron further show that their OHT estimates are in reasonable agreement with the sparse direct estimates made from hydrographic observations. This is in contrast with older heat transport estimates that had a similar total but required more ocean transport than could be supported by direct observations (Carrismo et al. 1985). In the older estimates, the atmosphere and ocean had roughly equal heat transport maxima. Trenberth and Caron show that the atmospheric heat transport dominates over most of the globe. Only close

Corresponding author address: Dr. Michael Winton, NOAA/GFDL, P.O. Box 308, Princeton University, Forrestal Campus, Princeton, NJ 08542.
E-mail: mw@gfdl.noaa.gov

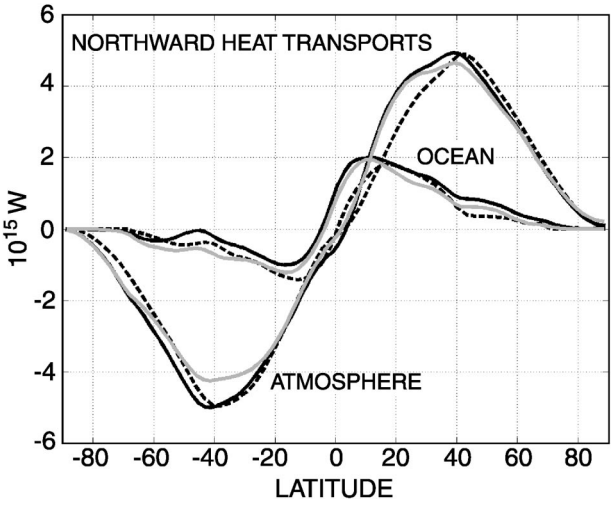

FIG. 1. Atmospheric and oceanic heat transports from observations (dashed lines) and the model AMIP experiments (AM2 dark lines, MCM light lines). The observational estimates are the average of the ECMWF- and NCEP-based estimates of Trenberth and Caron (2001; data available online at http://www.cgd.ucar.edu/cas/catalog).

to the equator are the AHT and OHT of comparable size.

Held (2001) has given a heuristic explanation for the greater role of the ocean near the equator and its reduction moving poleward. Consider the main heat-transporting circulations in the Tropics: the atmospheric Hadley cell and the shallow oceanic overturning. Both of these can be thought of as Ekman cells and they are driven by the same stress (neglecting land for the moment). Therefore, their mass transports are the same and their relative heat transports are determined by the stability of each medium. Near the equator, the ocean stratification is large but the convecting atmosphere has little moist stability. Consequently, the ocean transport is favored near the equator. Note that the appropriate stability for the atmosphere is moist stability because our atmospheric heat transport estimates include latent heat transport. The equatorward transport of water vapor in the trade winds works against the atmosphere's ability to transport moist energy poleward.

There is another scale for ocean heat transport convergence in addition to the atmospheric heat transport convergence: absorbed shortwave radiation (Held 1999). If there were no oceanic or atmospheric heat transport, and if the planetary albedo remained fixed, temperatures would adjust until the OLR equaled the absorbed shortwave locally. The net radiation would be zero everywhere. The absorbed shortwave is therefore a scale for *local* heat balance. According to ERBE, the regions from 40° to 90° in each hemisphere have about 13 PW of absorbed shortwave. Therefore, these regions receive more than twice as much heating from the sun as they do from atmospheric transport and their heating from oceanic transport is an order of magnitude smaller. Both scales indicate a small role for the ocean in high-latitude climate.

Suppose that the OHT were somehow eliminated from the climate system. Since both the AHT and the OLR respond to changes in temperature, we might imagine that temperatures would adjust to bring them into balance in a climate that is not too different than our current one. This adjustment can be tested in coupled climate models employing a mixed-layer ocean component. Such models are typically run using q fluxes, artificial sources and sinks of heat that represent the effect of missing ocean heat transport (Russell et al. 1985). Some studies have looked at the response to modified q fluxes (Rind and Chandler 1991; Sutton and Mathieu 2002). Clement and Seager (1999) performed an experiment with the Goddard Institute for Space Studies (GISS) AGCM where the q fluxes were entirely eliminated. The SST difference between their no-q-flux and q-flux experiments showed broad regions of cooling, particularly in the Northern Hemisphere and a narrow band of warming near the equator (an increase in tropical SST gradients). There was some enhancement of the cooling in near-ice regions of the Northern Hemisphere. Clement and Seager did not report on the response of the sea ice or the sea ice model used; however, a later study referring to the same experiment (Seager et al. 2001) notes that the ice model is nondynamic but nevertheless a large expansion of sea ice cover occurs when q fluxes are removed. Seager et al. perform a similar pair of experiments with the National Center for Atmospheric Research Community Climate Model 3 (NCAR CCM3) holding sea ice fixed at its annual mean. Their figure for the CCM3 January surface temperature change shows a similar pattern of equatorial warming and broad areas of cooling in the Northern Hemisphere.

Another test of the role of ocean heat transport comes from an experiment performed by Gregory and Mitchell (1997) with the HadCM2 coupled climate model. The current Hadley Centre climate model, HadCM3, runs stably without flux adjustments but its predecessor, HadCM2, employed heat flux adjustments that were responsible for about half of the ocean heat transport. Gregory and Mitchell performed an experiment with HadCM2 where the flux adjustments eliminated. The global mean SST dropped about 2°C in 100 years. Gregory and Mitchell pointed to an increase in low- and midlevel cloudiness as responsible for a relatively uniform cooling between 45°S and 45°N.

Finally, Poulsen et al. (2001) studied the role of the ocean in modeling the Neoproterozoic snowball earth events. GCMs have obtained different results trying to model these global glaciations with reduced solar luminosity and atmospheric CO_2 of that period. Poulsen et al. showed that two coupled simulations with different initial ocean conditions (modern and cold) did not result in global freeze-up while two mixed-layer simulations (with and without horizontal diffusion) became ice covered in a few decades. They point to the role of win-

tertime convective heat loss from the ocean near the ice edge as the mechanism for the ocean's constraining influence on sea ice. In this mechanism there is the potential for oceanic heat transport to have a disproportionate influence on high-latitude climate. The ocean may supply its heat at the optimal time and place to effectively oppose sea ice expansion. Lewis et al. (2003, manuscript submitted to *Paleoceanography*) show further that, since ocean temperatures have a minimum at seawater freezing temperature, intense cooling at the ice edge can reduce the ocean temperature gradient and, consequently, the OHT convergence, allowing ice expansion even with a dynamical ocean model. In their solution the reduction of OHT and the expansion of the ice edge go hand in hand. A similar effect has been shown to allow expansion of the polar halocline in cold climates even under reduced freshwater forcing (Winton 1997).

In this study we shall explore the role of ocean circulation in climate with two kinds of coupled models. The first is a conventional slab mixed layer that stores and releases heat seasonally but does not represent the effects of ocean circulation. The second is a novel approach where fixed fields of ocean currents are used to advect heat and salt. These currents are then modified to explore the role of circulation. Since the experiments are idealized and, hence, do not have observational comparisons, it will be useful to employ multiple models in order to determine which aspects of the solutions are robust and to gauge the range of possibilities. This strategy has been employed in many model intercomparison studies. The new Geophysical Fluid Dynamics Laboratory (GFDL) Flexible Modeling System allows coupled model components to be changed within the same model. We make use of this capability to use various combinations of two atmosphere–land and two sea ice models in conjunction with the two ocean components to form our coupled climate models. The next section presents details of the models and experimental designs. The third and fourth sections report the results from the two kinds of experiments. Section five presents conclusions.

2. The models and experiments

a. Atmosphere–land and sea ice models

GFDL's new Flexible Modeling System allows a ''plug-and-play'' capability for coupled model components. We take advantage of this by performing all of the experiments of this study in pairs; one with each of two atmosphere–land components. Our primary atmosphere–land component is a developmental version of the new GFDL model called AM2 (GFDL GAMDT 2003). AM2 is a B-grid model with 2.0° latitudinal and 2.5° longitudinal resolution and 18 vertical levels. The model has a diurnal cycle and radiative treatment of H_2O, O_3, CO_2, N_2O, CH_4, and four chlorofluorocarbons (CFCs). Moist convection is handled with a modified relaxed Arakawa–Schubert (RAS) mass flux scheme (Moorthi and Suarez 1992). The large-scale cloud scheme has three prognostic tracers: liquid, ice, and cloud fraction, which are treated following the parameterizations of Tiedke (1993), Rotstayn (1997), Rotstayn et al. (2000), and Jakob and Klein (2000). The vertical mixing scheme is a Mellor–Yamada 2.5 turbulence closure, so the mixing has a dependence upon stability. The land model component (Milly and Shmakin 2002) has five layers for temperature.

Our secondary atmosphere–land component is the Manabe Climate Model (MCM). This is an older atmospheric model that has been used extensively in greenhouse warming and other climate studies (Delworth et al. 2002). The MCM is a spectral model with R30 horizonal resolution, somewhat coarser than AM2, and 14 vertical levels. It does not have a diurnal cycle. The MCM uses a moist convective adjustment rather than a mass flux scheme for convection. Clouds are diagnosed based on relative humidity rather than prognosed. There is no stability dependence in the vertical mixing scheme. The land model does not have heat capacity.

The primary sea ice model we use in the experiments is GFDL's new IM2 sea ice model, a dynamical model using the elastic–viscous–plastic technique to implement a viscous–plastic rheology (Hunke and Dukowicz 1997). The thermodynamic treatment is similar to that of Semtner (1976) with two ice layers and one snow layer. The brine content of the upper ice is simulated rather than parameterized as in Semtner (Winton 2000). The model allows an arbitrary number of ice thickness categories; we use five, following the NCAR Climate System Model (CSM) sea ice model. The albedo scheme also follows the NCAR Community Sea Ice Model (CSIM4; Briegleb et al. 2002). This scheme has been shown to represent the major albedo regimes at the Surface Heat Budget of the Arctic (SHEBA) station: dry snow, melting snow, dry ice, ponded ice, and refrozen ice with light snow cover (Curry et al. 2001). A secondary sea ice model is used for comparison in the slab ocean experiments of the next section. This model is the same sea ice parameterization employed in the old GFDL climate simulations. The ice has a single no-heat-capacity layer. Snow and open water albedos are factored in based upon the surface temperature and thickness of the sea ice.

b. No-ocean-circulation experiments

Here we describe the design for the no-ocean-heat-transport experiments discussed in section 3. A coupled climate model with no ocean currents or heat transport is easily constructed by coupling the atmosphere, land, and sea ice components to a slab mixed-layer ocean. This ocean model will store and release heat seasonally but does not transport heat. In the long-term mean the

ocean surface heat flux must be zero, everywhere. We will use Atmospheric Model Intercomparison Project (AMIP) runs of the atmosphere–land models, forced with seasonally varying SST and sea ice observations, as the heat-transporting control experiments. When such a model is in radiative balance at the top, it will also have a zero net heat flux at the sea surface, and then the mean heat fluxes can be interpreted as an ocean heat transport convergence. This is, in some sense, the OHT that is compatible with both the model and the observed SSTs. Both the MCM and AM2 AMIP runs are within 1 W m^{-2} of net radiative balance, allowing this interpretation to be made. The use of AMIP controls is a shortcut around the usual procedure of diagnosing *q* fluxes in a run with restored SSTs and sea ice. When successful, the subsequent *q*-fluxed experiment recovers the climate of the AMIP experiment, although the variability may be larger.

We will interpret the differences between the AMIP runs and the non-flux-adjusted mixed-layer runs as stemming from the presence of ocean heat transport in the former. Therefore, it is important that the heat transports in the AMIP runs accurately depict those of the actual climate. Figure 1 shows the AHT and OHT for the AM2 model run in AMIP mode along with the average of the NCEP- and ECMWF-based estimates of Trenberth and Caron. Although locally there are discrepancies with the observations, globally the AM2 transports are in reasonable agreement and they capture the basic structure and differences in magnitudes of the transports seen in the observations. This is not the case for all atmospheric models run in AMIP mode. Gleckler et al. (1995) compare the implied ocean heat transports of 15 AMIP AGCMs. They find that the results are widely varying, with most of the models showing equatorward heat transport throughout the Southern Hemisphere. Gleckler et al. conclude that the differences between the models stem largely from differences in their cloud radiative forcing.

c. Variable ocean circulation experiments

Here we describe the design for the variable circulation experiments presented in section 4. Some studies have explored the response of simulated climate to freshwater-induced perturbations of ocean circulation (Manabe and Stouffer 1997; Vellinga and Wood 2002). These studies focus on the impact of thermohaline circulation heat transport while our interest here is in the impact of the total ocean heat transport. Another approach to representing variable ocean heat transport would be to use varying magnitudes of heat *q* fluxes (Rind and Chandler 1991; Clement and Seager 1999; Seager et al. 2001; Sutton and Mathieu 2002). However, from the experiments with the slab ocean below and the Poulsen et al. study discussed in the introduction, we expect that there will be variations in the sea ice edge. As noted by Poulsen et al., the sea ice edge is a region of OHT convergence. We would like to allow this OHT convergence to follow changes in the sea ice edge. For this reason, the *q*-flux approach has been passed over in favor of an approach that fixes currents and allows heat transport to adjust with the temperature field. In this approach, the ocean component of the coupled climate model is a transport or kinematic model. The model may be thought of as a full coupled climate model with the exception that it has fixed ocean currents. Ocean temperatures and salinities are freely varying but there will be no ENSO or thermohaline circulation variability, for example, as these involve dynamical ocean responses. A drawback of the kinematic ocean relative to the *q*-flux approach is that we introduce the long timescales of the full ocean depth and so we will, to some degree, be looking at climate transients. A drawback relative to freshwater-perturbed studies is that by specifying the ocean circulation we have eliminated circulation feedbacks.

The domain and currents for the kinematic ocean model come from the old GFDL climate model ocean initialization. Along with advection of heat and salt by these currents the model has vertical diffusion, convection, and Gent–McWilliams (GM) eddy mixing. The last two of these are sensitive to the evolving density structure of the model: the model can transition between stable and unstable vertical mixing. The vertical mixing formulation is as in the old GFDL climate model ocean component. A constant coefficient of 500 $m^2\ s^{-1}$ is used for the GM mixing. The ocean is initialized with Levitus temperatures and salinities. The experiments are run for 100 yr.

Six of these fixed-current experiments are performed: three with each atmospheric component. All of these experiments make use of the dynamic sea ice model. The three experiments with each atmosphere–land component consist of a control experiment and two companion experiments with ocean currents uniformly reduced and increased by 50%.

3. Results from the mixed-layer coupled models

The slab ocean experiments are initialized with observed SSTs and sea ice. Figure 2 shows the evolution of global mean surface air temperature, sea ice extent, and reflected shortwave. The temperature responses range from modest cooling in the MCM–thermodynamic sea ice case to extreme cooling in the dynamic ice experiments with both atmosphere–land components. In the latter, the temperature falls from near the observed values to 0°C in a little more than two decades and has not equilibrated at the end of the experiment. Both experiments with the dynamic ice model experience unstable growth of sea ice. The thermodynamic ice model experiments both equilibrate but with sea ice cover that is several times the observed (about 24×10^{12} m^2). Figure 2 shows that in spite of its large sea ice cover the MCM–thermodynamic ice experiment has a global

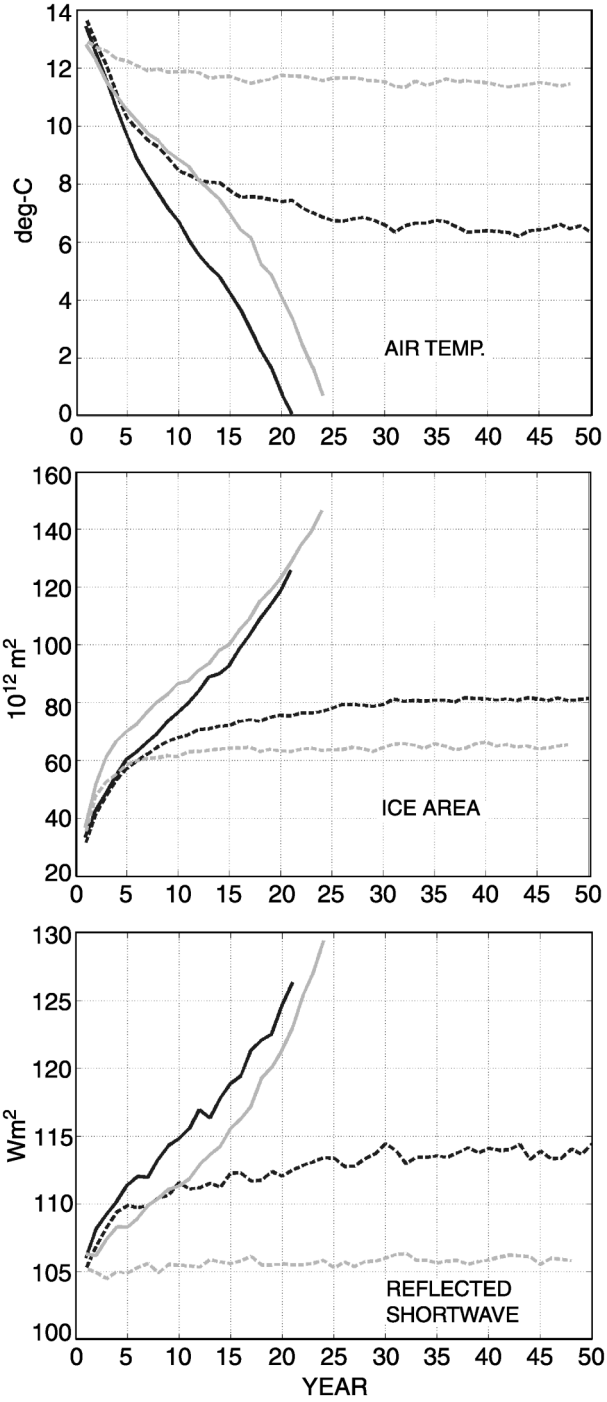

FIG. 2. Mixed-layer model experiments for AM2 (dark lines) and MCM (light lines): (top) global mean air temperature, (middle) global sea ice extent, and (bottom) global mean reflected shortwave. The experiments with dynamic sea ice are solid lines and those with thermodynamic sea ice are dashed.

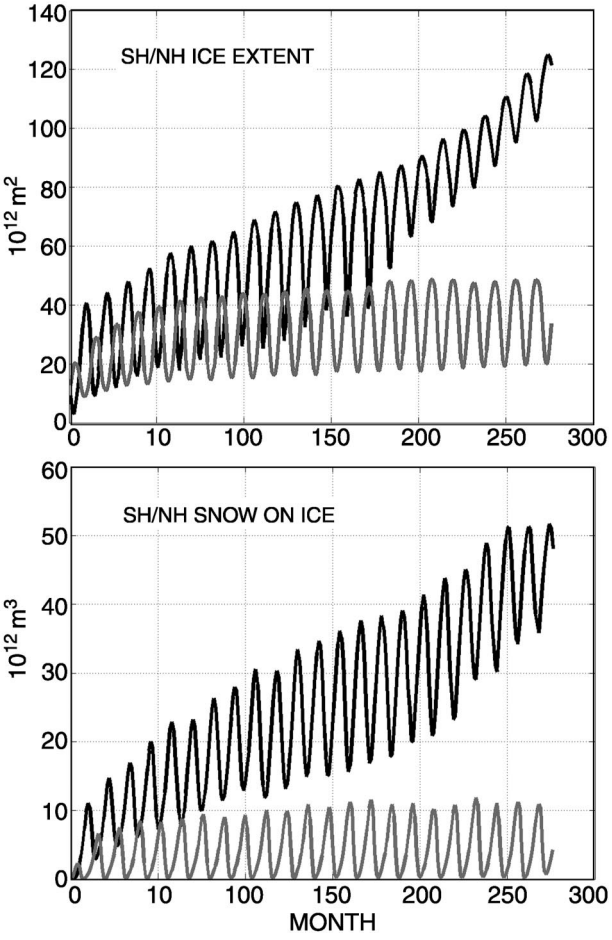

FIG. 3. AM2 mixed-layer model experiment with dynamic sea ice model: Southern (dark lines) and Northern (light lines) Hemisphere (top) sea ice extent and (bottom) snow on sea ice.

reflected shortwave similar to that of its AMIP control experiment (about 103 W m^{-2}). The other three experiments have substantially increased reflection. The unstable MCM run develops more sea ice but less shortwave reflection than its AM2 counterpart, indicating that other factors also contribute to the shortwave changes. Taken as a group the experiments suggest that ocean heat transport is an important constraining influence on sea ice extent and also has some warming influence.

There are reasons to expect dynamic sea ice to be more expansive than nonmoving ice. In the westerly band the Ekman drift will favor equatorward motion of the ice. Even where the mean forcing is not favorable to equatorward motion, ice internal forces oppose concentration of the pack while freely allowing dilation. A more important aspect of the dynamic model for the unstable behavior of the experiments, however, seems to be presence of a snow layer. Figure 3 shows seasonal Northern and Southern Hemisphere sea ice extents for the AM2–dynamic ice experiment. After an initial adjustment, the Northern Hemisphere sea ice extent is slowly growing near three times its observed value. The Southern Hemisphere sea ice extent grows unstably. Figure 3 also shows the snow volume on the southern and northern packs. The northern snow melts complete-

ly away every summer while the southern pack develops a perennial snow cover. The high summer albedos prevent the nearly complete summer melt back of the southern ice that occurs in today's climate. In this way the summer snow protects its own platform. But perennial snow raises a concern for the simulation: since the sea ice model does not age snow, the snow cover may be unrealistically reflective. The sea ice model was not designed to handle perennial snow on sea ice. Consequently, the instability of the southern sea ice in the dynamic ice experiments may be the result of an unrealistic treatment of snow. Less attention has been paid to snow on sea ice than to other aspects of the model because there is so little snow-covered ice in the summer in today's climate. Snow on the northern pack melts rapidly away, partly under the influence of the warm temperatures of air warmed over the landmasses surrounding the Arctic Ocean. In the Southern Hemisphere, the ice pack melts back, eliminating the platform for snow. Much of the Southern Hemisphere sea ice originates as snow and is converted to sea ice as it is pushed below the waterline (Eicken et al. 1994). This effect, which is also present in the dynamic ice model, serves to limit the snow thickness on the sea ice. The validity of the unstable solutions depends upon the details of the snow treatment and other poorly known factors, oceanic snowfall among them.

In general, the dynamic ice model is a more physical representation of the sea ice and we would prefer to use it for this experiment where sea ice response is clearly important. When it is used in conjunction with the mixed-layer ocean, however, the climate change in the model is so extreme that it becomes difficult to interpret and analyze. The large increase in sea ice in these experiments is unexpected based on the smallness of ocean heat transport convergence relative to atmospheric convergence and absorbed shortwave in the high-latitude regions. It is worth emphasizing that these unstable solutions were obtained with a modern solar constant and CO_2 levels, unlike the Poulsen et al. results, which made use of solar forcing that was 95% of the present value and a CO_2 level of 140 ppmv.

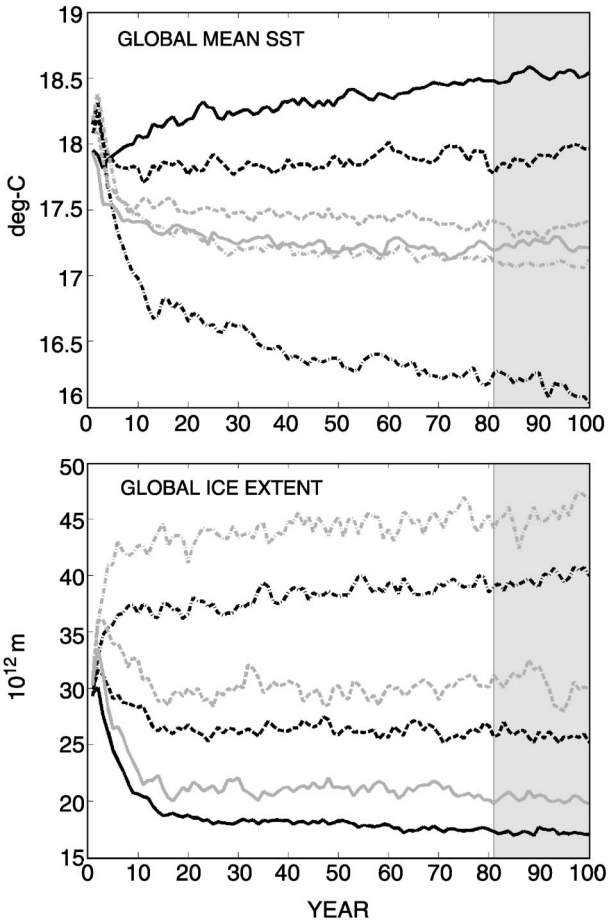

FIG. 4. Spinup of global (top) mean SST and (bottom) sea ice extent for the six fixed-current experiments: AM2 (dark lines) and MCM (light lines). Slow currents are dashed–dotted lines, control currents are dashed lines, and fast currents are solid lines.

4. Results from the fixed-current coupled models

a. Spinup of the experiments

Figure 4 shows time series of global mean SST and sea ice extent for the six experiments. The relationships between the experiments set up in a few decades and are stable over the course of the runs, although the models are not in steady state at the end of the integrations (this is particularly true of SST). Although the MCM-based model experiments have somewhat more sea ice than their AM2 counterparts, the relationships between the experiments are similar in the two models. The slow current experiment has the most sea ice, the fast current model the least, and the control is in the middle. For both models, the increase in sea ice between control and slow currents is greater than the decrease between control and fast current experiments. None of the experiments show unstable ice or even ice extents nearly as large as the least icy of the mixed-layer experiments. Apparently, even a small amount of ocean circulation places a strong constraint on sea ice extent. Setting aside concerns about perennial snow albedo, these results, in conjunction with the dynamic ice results of the previous section, are similar to those of Poulsen et al. but show that ocean dynamics plays a critical role in stabilizing sea ice extent in *today*'s climate as well as that of the Neoproterozoic.

The similarity between the sea ice extent sensitivity of the models is contrasted by the differences in global mean SST sensitivity shown in Fig. 4. The SST plot shows that the MCM-based models have only small differences, while there is a large cooling going from control to slow currents and a much smaller but significant warming from control to fast current experiments with the AM2-based models. The 2°C cooling of

TABLE 1. The 100-yr average ocean heat uptake (W m^{-2}, earth surface) for the six fixed-current experiments.

	50%	100%	150%
AM2	0.81	1.43	2.13
MCM	0.62	0.51	0.67

SST in response to a 50% reduction in current strength is roughly consistent with the HadCM2 SST cooling of a similar magnitude in response to removal of the heat flux adjustments that transported about half of the total heat. The heat transport in the reduced-current AM2 experiment is changing roughly in proportion to the current weakening. The heat export from the region 15°S–15°N, for example, was reduced by 48% from the control.

A question arises concerning the interpretation of the climate changes shown in Fig. 4. Are they driven by changes in ocean heat transport or by changes in ocean heat storage? By altering the currents we have altered the transport mode of the ocean but also introduced a storage mode. Consider that the cold water underlying the equator is brought there by advection from high latitudes. If currents are weakened, we expect that this deep water will warm diffusively, reflecting more the local surface conditions. To the extent that the SST is pinned by other processes, the ocean will take up heat and act as a cooling influence on the surface. Likewise, increasing the circulation should result in a release of heat from the ocean warming the surface. Is this process driving the climate changes we see? Table 1 shows the average heat uptake over the 100-yr duration of each experiment. They are positive for all of the experiments (both AMIP runs had a net downward radiative flux of about 0.5 W m^{-2}). If the storage mode were dominating the solutions, we would expect that the uptake would be similar between experiments of similar current strengths and that the weak current cases would have the largest uptake and the strong current cases the smallest. Instead the MCM experiments have nearly the same uptake, and of the AM2 experiments, the slow current case has the least uptake and the fast current case the most. This seems to be evidence for climate change–driven storage rather than storage-driven climate change in AM2 model. In the AM2 experiments greater storage is associated with warmer global SST as if the climate change were penetrating into the ocean much as in a greenhouse warming experiment. Although the adjustment of the thermocline to a new equilibrium must be occurring, it is apparently not dominating the model solution in these century-long experiments.

b. Comparison of climatologies

Climatologies for the six experiments are constructed from the last 20 yr of each 100-yr integration. The climatological seasonal sea ice extent plots (Fig. 5) for the two hemispheres show many similarities between the responses of the two models. Both models have a larger sensitivity of southern than northern sea ice and a larger response in the winter season in both hemispheres. The enhanced sensitivity to a reduction in currents is evident in both hemispheres, both seasons, and both models with the exception of the Northern Hemisphere summer in the MCM model. In all of the experiments, there is a large melt back of the southern sea ice in summer, eliminating the platform for perennial snow that was so worrisome in the no-OHT experiment. As a percentage of the control the MCM-based model has a larger response than the AM2 in the south and a smaller response in the north. The total response, however, is the same in the two models to within 5%.

The greater sensitivity of the winter sea ice extent is evidence for the importance of convective upward heat flux from the ocean in constraining the sea ice edge as this flux occurs in the wintertime. This heat flux is modulated by changes in the halocline that occur as the currents are varied. Table 2 shows the fraction of the high-latitude oceans that have annual haline stratifications in excess of 0.5 psu. This value was chosen because the Southern Ocean is marginally stratified by this measure and the halocline there is known to leak some heat upward in the wintertime (Martinson and Iannuzzi 1998). In both models there is an increase in halocline cover as the currents weaken, protecting the ice from upward oceanic heat fluxes in a larger region. The change is promoted both by the reduction in heat advection that drives vertical instability and mixing, and by the reduction of freshwater flushing out of high latitudes.

The annual mean surface air temperature (SAT) difference between the fast and slow current experiments for the two models (Fig. 6) is similar in that there is warming of the mid- and high-latitude oceans, which is intensified in the regions of sea ice retreat. In the MCM-based model, cooling dominates the low-latitude oceans, while in the AM2-based models there are only small regions of cooling near the equator but substantial warming in the subtropical gyre regions and also over land. The Clement and Seager (1999) SST difference (their Fig. 10) is similar to these patterns except for a change of opposite sign in the Southern Ocean. The global mean SAT response of the two models (Table 3) is quite different. The MCM-based model has only a small change across the range of experiments (0.6°C) while that of the AM2-based model is almost six times larger. Both models show a larger cooling with reduced currents than warming with increased currents.

The zonal mean SST for the two models (Fig. 7) shows a flattening of the high-latitude profile with slower currents and expanding sea ice. In the Tropics, the profile flattens with faster currents, reducing the gradient. This comes about in different ways in the two models. In the MCM-based model, the maximum SST is reduced as the currents strengthen, while in the AM2-based model the maximum SST stays the same but there

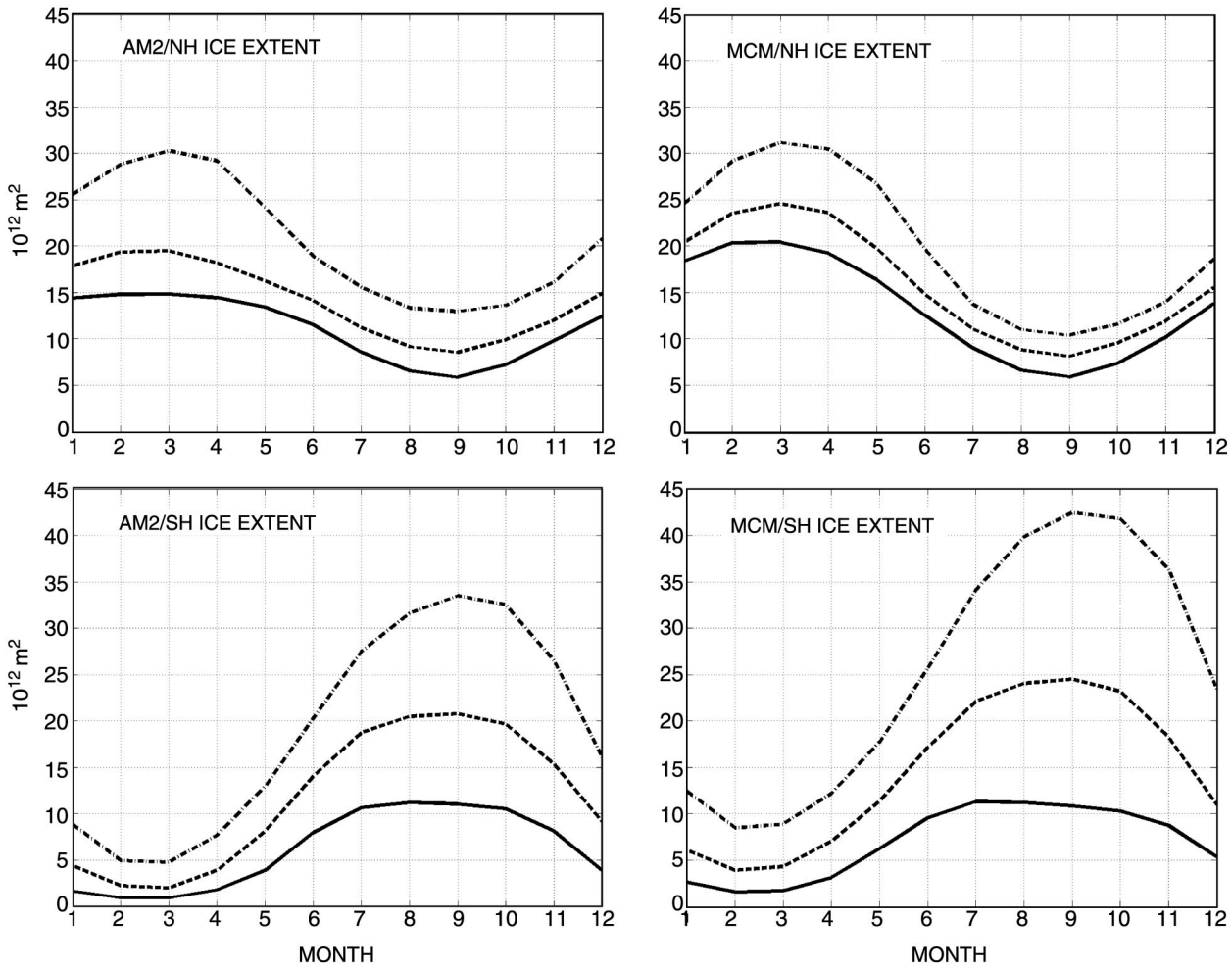

FIG. 5. Seasonal sea ice extent for the (top) Northern and (bottom) Southern Hemispheres for the two fixed-current models: (left) AM2 and (right) MCM. Slow currents are dashed–dotted lines, control currents are dashed lines, and fast currents are solid lines.

is warming in the off-equatorial trade wind bands. The extratropical Northern Hemisphere shows a larger cooling with slower currents than the Southern in both models, but this effect is much more pronounced in the AM2-based model. Enhanced response of the Northern Hemisphere SST was also a feature of the Clement and Seager experiment. There does not appear to be strong intrahemispheric coupling between SST and sea ice extent, as the southern sea ice extent is more responsive than the northern in both models.

Now we return to the question, posed in the introduction, of how AHT and net radiation would compensate for changes in OHT. First, note that changing the current strength has been an effective way to change the OHT. In both models the OHT scales with the currents—the difference in heat export from 15°S to 15°N between the perturbation and control experiments range from 35% to 48%. Both models show (Fig. 8) a flattening of OHT toward the poles, particularly in the Northern Hemisphere, as currents are reduced. This may be partly a result of the high-latitude SST flattening accompanying ice expansion. The MCM-based model AHT actually overcompensates for the decrease in OHT at 40°N and 40°S, increasing the total energy transport into these regions. The AM2-based model does not have AHT compensation for the reduction of OHT at 40°N and 40°S. To a lesser degree this difference between the models is also present at 20°N and 20°S. But the AM2-based model seems to have a greater response to the OHT changes very near the equator.

Now we look at the sensitivity of wind stress over the ocean (Fig. 9). This is important because it can tell

TABLE 2. Area of ocean between 40° and 90° latitudes with 0–300-m annual mean haline stratification greater than 0.5 psu (10^{12} m^2) for the six fixed-current experiments.

	50%	100%	150%
AM2	94%	81%	41%
MCM	88%	57%	25%

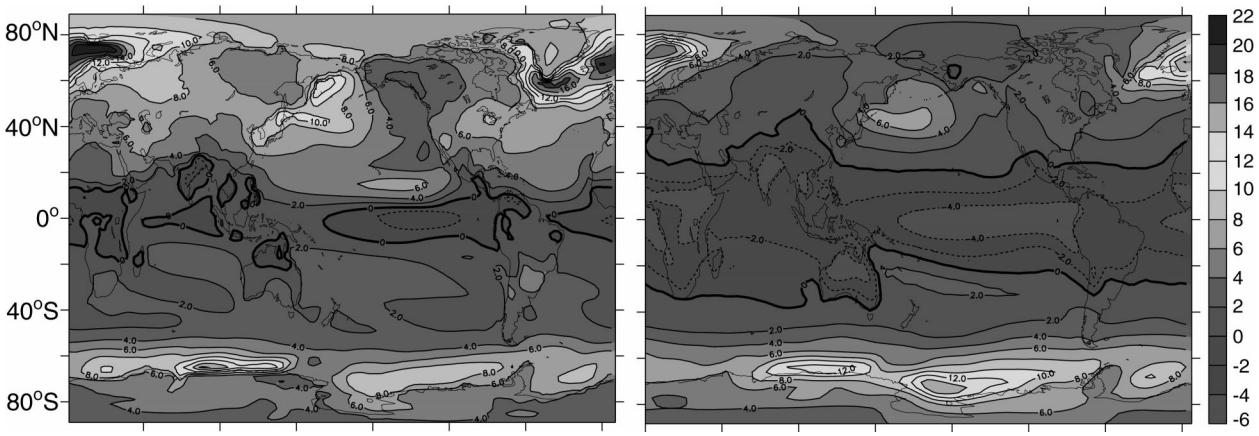

FIG. 6. Annual mean surface air temperature difference between 150% and 50% of current cases of the two fixed current models. (left) AM2 and (right) MCM.

us whether the coupled system will have a negative feedback that is not represented in these fixed-current ocean experiments. That is, when OHT is reduced, will the winds respond by driving the ocean in a manner that would increase the OHT in a fully coupled system? The models agree that zonal mean wind stress increases with decreasing ocean circulation but the pattern of wind stress response is quite different. The primary response of wind stress in the AM2-based model as currents weaken is a strengthening and equatorward shift of the trades and the Northern Hemisphere westerlies. The stronger trade stresses in the AM2-based model indicate a spinup of the atmospheric Hadley cell. The MCM-based model also shows some tendency for the trade stresses to increase but the main response is a large strengthening of the Southern Hemisphere westerly stresses, a region where the stress is unchanged in the AM2-based model. The differences suggest that fully coupled models based on the two atmospheric components might have different adjustments to ocean circulation biases. An AM2-based model might adjust the strength of its shallow tropical cell and Northern Hemisphere gyres, while an MCM-based model might adjust by modulating the strength of its deep North Atlantic overturning cell through the connection between Southern Ocean wind stress and deep Atlantic overturning (Toggweiler and Samuels 1995; Gnanadesikan 1999).

Figure 10 shows the annual mean precipitation for the six experiments. Both models have split intertropical convergence zones (ITCZs) in the Pacific with control and increased currents associated with the upwelling of cold water along the equator and the overlying descent

TABLE 3. Global mean surface air temperature (°C) for the six fixed-current experiments.

	50%	100%	150%
AM2	11.1	13.7	14.6
MCM	11.6	12.2	12.2

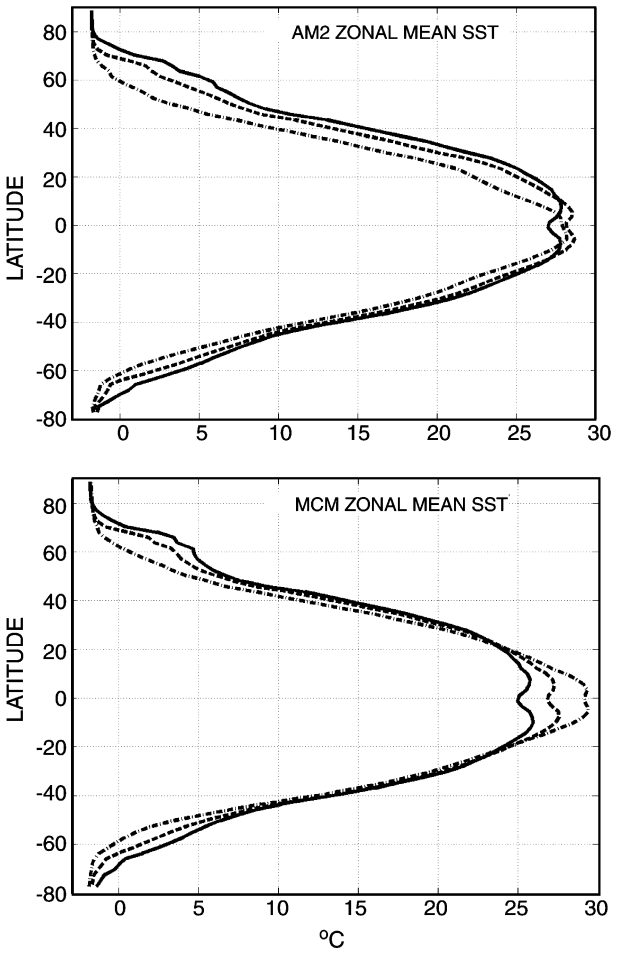

FIG. 7. Zonal mean SST for the two fixed-current models: (top) AM2 and (bottom) MCM. Slow currents are dashed–dotted lines, control currents are dashed lines, and fast currents are solid lines.

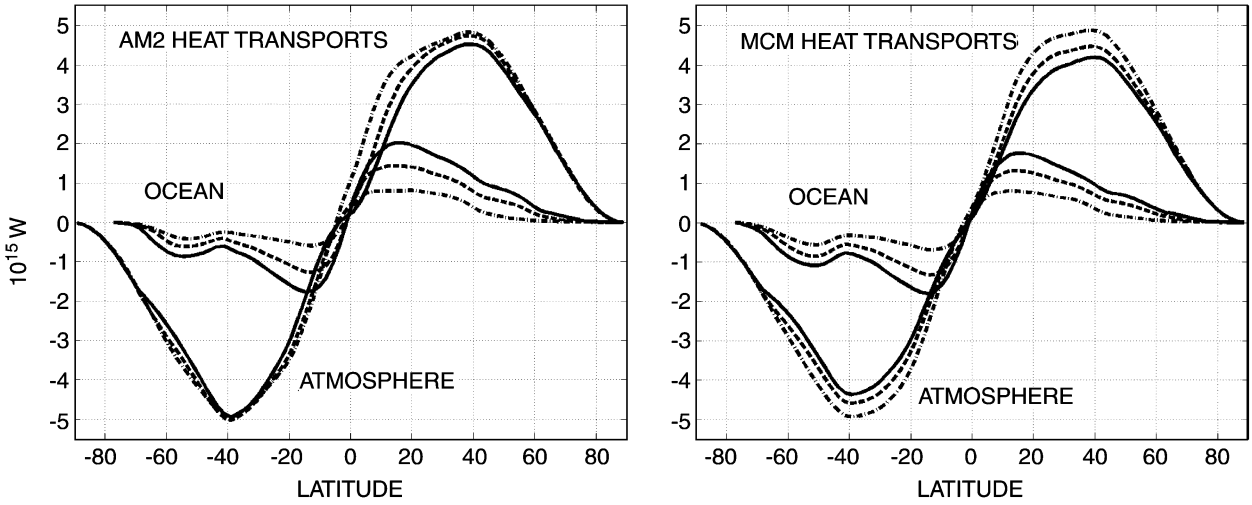

FIG. 8. Northward atmospheric and oceanic heat transports for the two fixed-current models: (left) AM2 and (right) MCM. Slow currents are dashed–dotted lines, control currents are dashed lines, and fast currents are solid lines.

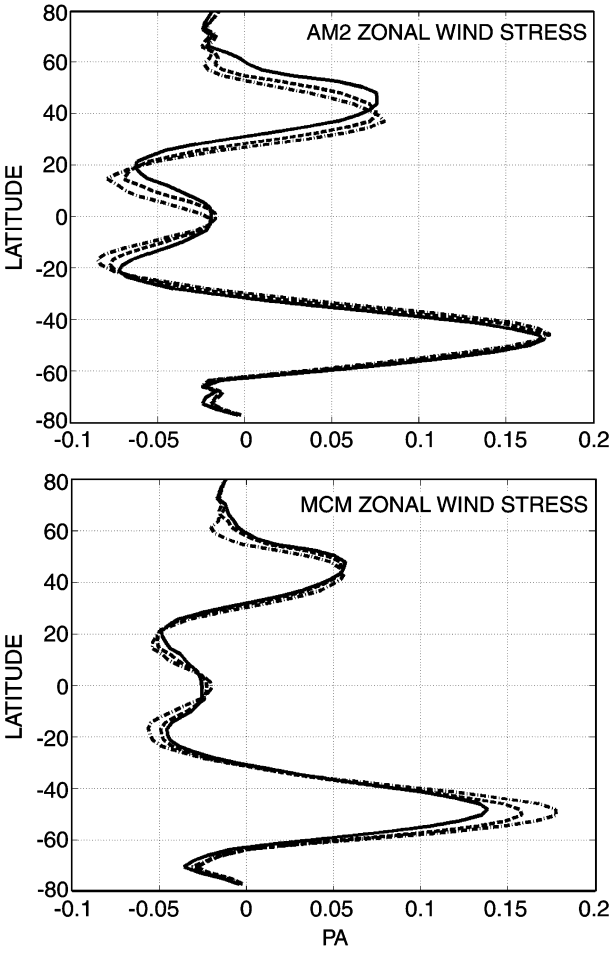

FIG. 9. Zonal mean wind stress on the ocean for the two fixed-current models: (top) AM2 and (bottom) MCM. Slow currents are dashed–dotted lines, control currents are dashed lines, and fast currents are solid lines.

in the atmosphere. With reduced currents both models shift to a single Pacific ITCZ in the Southern Hemisphere and develop a large region of descending air in the North Pacific. The MCM-based model has a greater proportion of its precipitation over land than the AM2-based model does in all cases. There is a tendency for the MCM deep convection to be over or near Indonesia and so it has a smaller shift of precipitation eastward in the South Pacific ITCZ with reduced currents. The MCM maintains more Walker circulation as currents are reduced and this may partly account for the reduced sensitivity of its trade winds to circulation strength seen in Fig. 9. The dry subtropical oceanic regions with less than 2 mm day^{-1} precipitation expand in both models as the current strength is reduced and off-equatorial descent increases. The westward expansion of the dry zone is particularly large in the North Pacific in the AM2-based model where it grows from the eastern half of the basin in the increased currents experiment to cover the breadth of the basin in the reduced-currents experiment.

c. Shortwave budgets and cloud feedbacks

Now we pursue the reason for the much larger response of global mean temperature in the AM2-based model (Table 3). The shortwave budgets of the two models show a likely cause for the difference. In Table 4 the top-of-atmosphere absorbed shortwave budget of the two models is shown in total and for three regions: the ocean poleward of 40° in both hemispheres, the ocean equatorward of 40°, and over land. In the ocean 40°–90° region the change with current strength is similar between the two models: the shortwave absorption increases with increased currents by a little less than 10^{15} W in the AM2-based model and a little more in the MCM-based model. The sensitivity of the 40°–40°

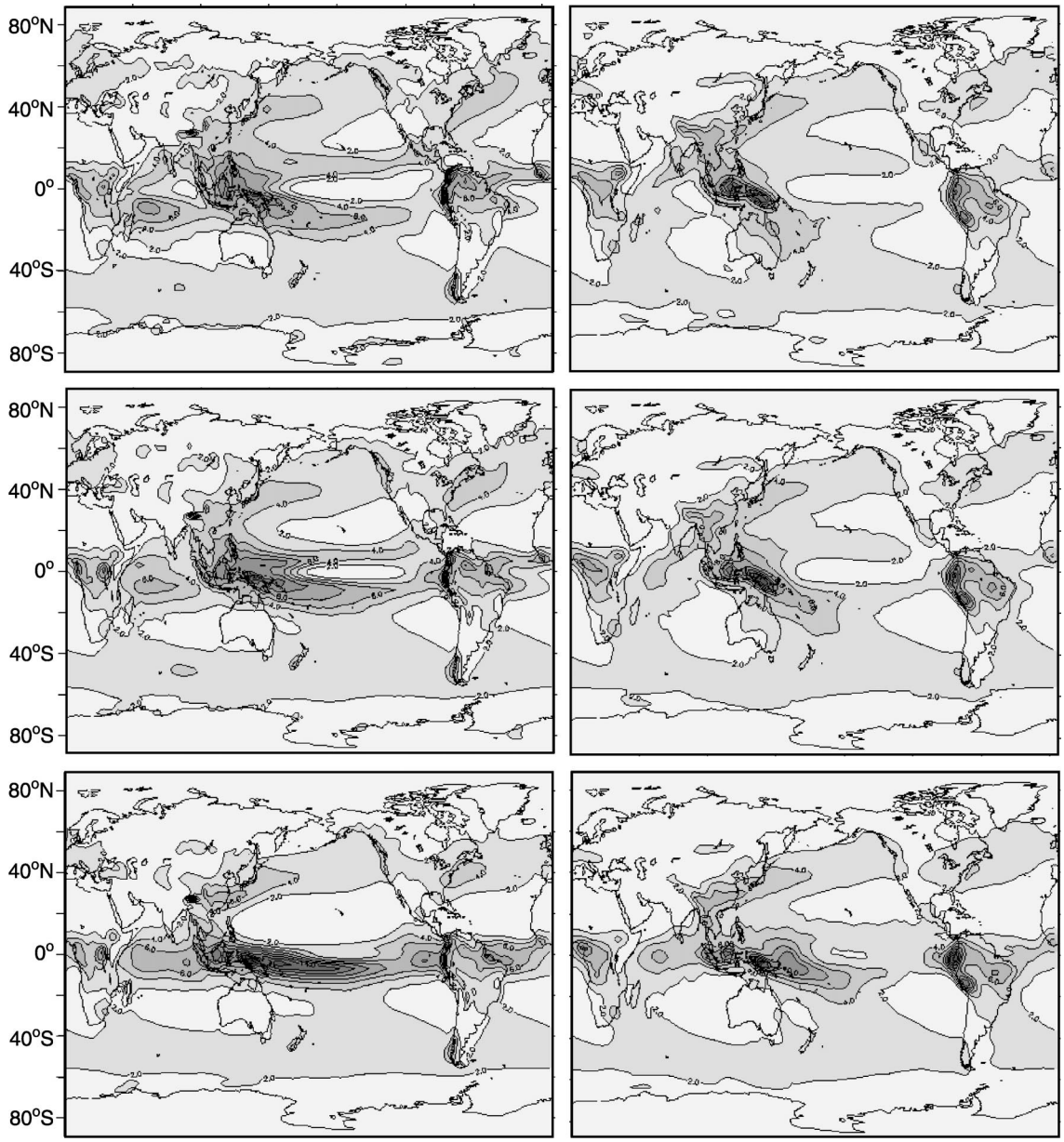

FIG. 10. Annual mean precipitation (mm day^{-1}): (left) AM2- and (right) MCM-based experiments; (top) 150% currents, (middle) 100% currents, and (bottom) 50% currents.

TABLE 4. Regional and total absorbed shortwave (PW) for the six fixed-current experiments.

	AM2 50%	AM2 100%	AM2 150%	MCM 50%	MCM 100%	MCM 150%
Land	33.08	33.29	33.30	32.54	32.34	32.20
Ocean 40°–40°	69.24	70.32	71.02	70.04	69.39	69.05
Ocean 40°–90°	17.49	18.04	18.35	17.15	17.97	18.27
Total	119.81	121.65	122.67	119.73	119.70	119.53

ocean region is opposite in the two models. The AM2-based model reinforces the 40°–90° ocean changes by absorbing more shortwave in 40°–40° with stronger currents. The increase is about twice that in the 40°–90° ocean region. The MCM-based model has a decrease of about 10^{15} W of shortwave absorption with stronger currents that nearly cancels out the 40°–90° changes. Both models have small changes in the land region absorption that follow the changes in their respective 40°–40° ocean regions. The global result is almost no change in the shortwave budget for MCM but a nearly 3×10^{15} W increase from slow to fast currents in the AM2-based model.

TABLE 5. Cloud cover by height category for the six fixed-current experiments.

	AM2 50%	AM2 100%	AM2 150%	MCM 50%	MCM 100%	MCM 150%
Low	43.8	40.8	39.4	31.1	33.3	34.9
Middle	21.5	20.6	20.2	13.6	13.9	14.2
High	35.7	35.9	35.2	27.8	27.4	27.2

While changes in snow cover contribute to the shortwave changes over land and sea ice cover to the changes in the ocean region poleward of 40° in the models, the equatorward of 40° ocean region changes must be due to cloudiness since this region is virtually ice free in all of the experiments. This motivates us to look at the global cloud cover.

Cloud cover in total and by height category is shown in Table 5. The global low cloud cover has the largest response, changing by about 4% in the two models over the range of experiments. The changes are in the opposite sense: increasing clouds accompany decreasing currents in the AM2-based model but increasing currents in the MCM-based model. The increase in low cloudiness in the AM2 model is in qualitative agreement with the increase in low cloudiness reported by Gregory and Mitchell (1997) in the HadCM2 model when the heat-transporting flux adjustments were removed. The midlevel clouds have smaller changes echoing the low cloud changes in the two models. Both models have fairly stable high cloud amounts. The two model controls differ considerably in the amounts of the low, middle, and high clouds but have similar radiation budgets. The cloud radiative properties compensate for the differences in cloud amounts to produce similar global radiative budgets. Of the three height categories, low clouds are especially important for the energy balance of the earth because, unlike higher clouds, they have very little impact on the OLR to counteract their strong impact on shortwave absorption. Hartmann et al. (1992) show that the low cloud cover of the earth exerts a cooling influence of 15 W m^{-2}.

But why are the low clouds changing with ocean circulation intensity? Insight into this comes from Klein and Hartmann (1993) who found a strong empirical relationship between the seasonal low stratus cloud amounts observed from ships and the lower atmospheric stability, the 700 mb–surface potential temperature difference, in the marine stratus regions. They also showed that interannual variations of the two quantities at a weather station off the California coast were strongly correlated.

Do the low clouds in the model have relationship with lower atmospheric stability like that observed by Klein and Hartmann? Zonal and monthly averaged 1000–700-mb stability and low cloud amounts are shown in the scatterplot for the oceanic bands between 40°S and 40°N in Fig. 11. The AM2 model (black dots) has a positive relationship between these two quantities as in the observations (70% explained variance). There is little relationship (38% explained variance) in the MCM-based model but the fit has a negative slope. Also shown are the 40°–40° ocean means for the three current strengths in the two models. Both models have an increase in lower atmospheric stability with decreasing current strength. The stability increase is considerably larger in the MCM-based model. Both models associate a change in mean cloudiness with the stability change that is roughly consistent with their seasonal relationships in the control experiments. So the models have stability

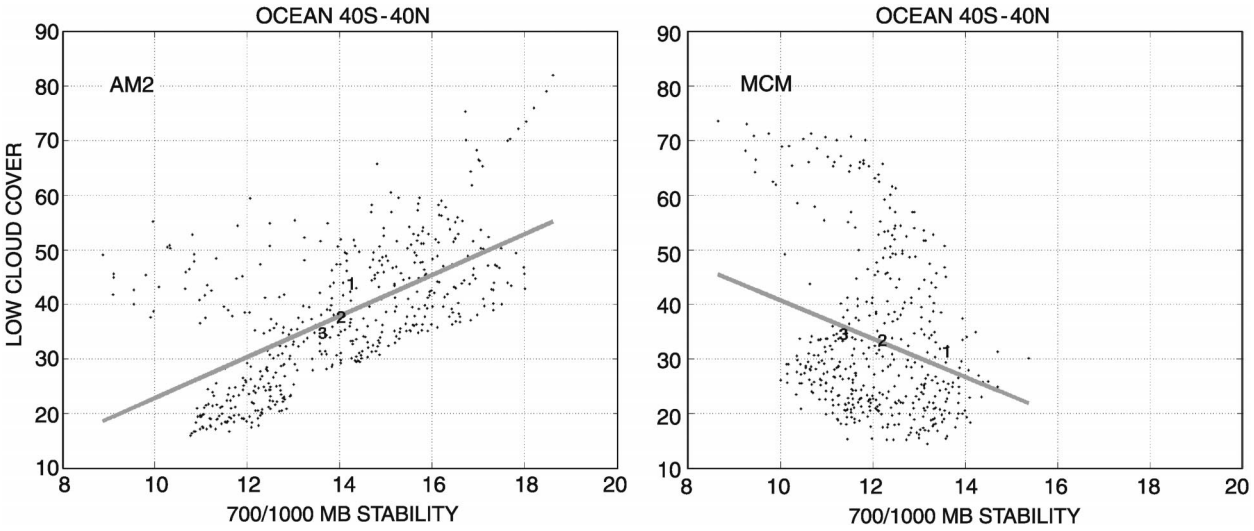

FIG. 11. Zonal and monthly mean stability and low cloud cover for the two fixed-current model control cases (dots) and regression (light line) for (left) AM2 and (right) MCM. The numerals denote the 40°S–40°N oceanic means for the weak current, control current, and strong current experiments (1, 2, and 3, respectively) with each model.

changes of the same sign but low cloud changes of opposite sign.

Atmospheric stability affects the low cloud amount by inhibiting entrainment of dry air above the boundary layer that reduces the relative humidity and suppresses cloud formation. But low cloudiness also affects atmospheric stability by shielding the surface from solar warming, reducing the SST. For this reason, it is difficult to point to either the low cloud or the stability as a cause for the other. The fact that the MCM-based model has the same stability response to ocean circulation intensity as the AM2-based model, in spite of having low cloud changes that oppose the stability changes, suggests that the stability changes are an inherent response to ocean circulation intensity.

There is a clear physical reason for the increase in atmospheric stability that accompanies a decrease in ocean circulation. It is illustrated nicely by simple two-box models of the tropical atmosphere such as the one used by Clement and Seager (1999). The two boxes represent the ascending (precipitating) and descending branches of the tropical atmospheric overturning. In this class of model, the free atmospheric temperature is required to be the same in both boxes and the atmospheric overturning is determined from the energy balance of the atmosphere: basically, condensation heating balancing long wave cooling. Clement and Seager couple their two atmospheric boxes to mixed-layer ocean boxes. They set the oceanic mass overturning (mixing between the mixed-layer boxes) to be a factor γ times the atmospheric mass overturning. As this factor is reduced from 1, the SST difference between the boxes increases. Since the air above the boundary layer in the cold pool box is warm pool air that has risen along a moist adiabat and descended over the dry pool, the SST difference is translated, fairly directly, into cold pool atmospheric stability. Clement and Seager have also built into their model a relationship between stability and low cloud in the cold pool based on the Klein and Hartmann (1993) regression line. Consequently, there is more low cloud and more shortwave reflection when γ is small and the SST gradient and atmospheric stability are large. This leads to cooling of both the warm and cold pool SSTs—a cooling of the entire Tropics. This basic mechanism tying ocean circulation, SSTs, lower atmospheric stability, and low cloudiness appears to be active in the AM2-based model as well. The AM2 model, however, has stability-dependent mixing and a prognostic cloud scheme so it is able to simulate the low cloud–stability relationship rather than employing it as an assumption. The absence of these features in the MCM model likely accounts for its inability to simulate the relationship.

But what then explains the reduction of low cloud with ocean circulation in the MCM-based model? Since clouds are diagnosed based on relative humidity in MCM we look at the relative humidity change in the experiments. The zonal mean relative humidity change for the strong minus weak current experiments is shown for the two models in Fig. 12. Both models show that increased ocean circulation is associated with a tripolar pattern of relative humidity changes with decrease near the equator and increases in the subtropics. In the MCM-based model, this pattern extends to the surface and the horizontal distribution of low cloud changes in that model follow this relative humidity pattern. Clement and Seager (1999) show the zonal mean change relative humidity between their no-*q*-flux and *q*-flux GISS GCM experiments (their Fig. 9). Their pattern generally agrees with the patterns shown here. In the same figure they also show the zonal mean atmospheric temperature changes between the experiments and these indicate that tropical stability is increasing as it is in the AM2- and MCM-based models. The three models are in qualitative agreement on the changes in SST gradient, lower atmospheric stability, and relative humidity but translate these differently into changes in low cloud and absorbed shortwave.

5. Conclusions

In spite of the smallness of oceanic heat transport relative to atmospheric, these experiments suggest that ocean circulation has a profound influence on climate. This influence is mediated by the special role that the ocean plays in the formation of radiatively important sea ice and low oceanic cloudiness. The experiments indicate that ocean circulation warms the climate by reducing both the sea ice extent and the low oceanic cloud cover.

The simulations without ocean heat transport all develop large ice packs. The precise behavior is sensitive to details of the sea ice formulation in a way that is not seen in simulations of the modern climate: with a modern dynamic ice component the no-ocean-heat-transport models develop unstable growth of sea ice. In the variable ocean circulation experiments, even with ocean currents reduced by 50% from control, the ice is stabilized at extents less than twice observed in both models. The ice extent is reduced by about 56% in both models as the currents are increased from 50% to 150% of the control experiment values. This sensitivity occurs in the MCM-based model in spite of compensation of atmospheric heat transport for the reduction of ocean heat transport into the regions between 40° and the poles. The MCM experiments have more ice than the AM2 experiments in each of the fixed-current cases, indicating that sea ice extent *does* have some sensitivity to the atmosphere and/or land formulations. The particular aspects of the atmosphere–land simulation that are influential in determining the sea ice extent remain to be explored. The mechanism for the ocean's strong role in constraining the ice seems likely to involve the upward convective flux of heat in the wintertime, as the wintertime maximum ice is more sensitive to the ocean current strength than the summertime minimum. Changes in the extent of the halocline vary with current

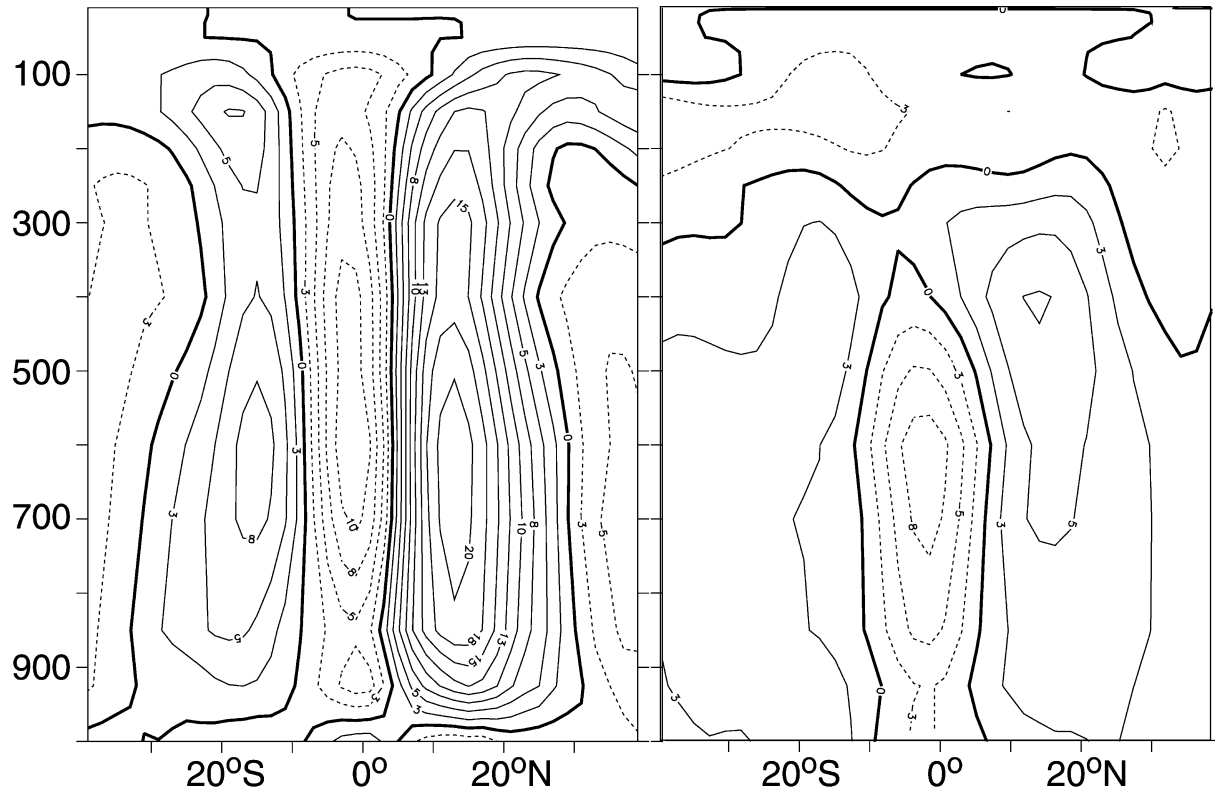

FIG. 12. Zonal mean relative humidity difference for the 150% currents minus the 50% current cases of the fixed-current experiments: (left) AM2 and (right) MCM.

strength in such a way as to encourage the sea ice extent changes. And yet other factors must also be involved as the MCM model has less extensive haloclines but more extensive sea ice in all cases.

The atmospheric heat transport response to reduction in currents differed between the models. The MCM-based model increased its transport into high latitudes to compensate for the reduction in oceanic transport while the AM2-based model did not. In fact the MCM-based model atmosphere overcompensated for the reduction in OHT across 40°S and 40°N so that the total energy transport into these regions was increased with decreasing ocean circulation. The low-latitude atmospheric heat transports were more responsive in the AM2 case.

The models have similar responses of SST gradients, atmospheric stability, and relative humidity to ocean circulation strength, but their different physical formulations result in different low cloud, planetary albedo, and global temperature changes. Because the AM2-based model is able to simulate a seasonal relationship between low cloudiness and stability similar to the observed and because its cloud response is consistent with this relationship, its prediction for the cloud changes are preferred here as more credible. Clement and Seager (1999) report that the low cloud simulation of the GISS model that they use is unsatisfactory and does not have the low cloud–ocean heat transport relationship found in their box model. The sensitivity of the GISS model that they use appears to resemble that of the MCM-based model used here while their box model is in agreement with the AM2-based model of this study.

The mechanism that changes low oceanic cloudiness with ocean circulation in the AM2-based GCM is well characterized by the simple model of Clement and Seager. Increased ocean circulation reduces the low-latitude SST gradient and, hence, the stability of the tropical atmosphere. In the AM2-based model, low clouds and atmospheric stability have a seasonal relationship similar to that found in observations by Klein and Hartmann (1993). In the model, this relationship also carries over to ocean circulation induced climate change and accounts for its low cloud sensitivity.

Acknowledgments. I wish to extend my thanks to my many GFDL colleagues who participated in the development of the component models and the coupling infrastructure used in this study. This paper has benefited from reviews by Tony Broccoli, Isaac Held, Steve Klein, Andrew Weaver, and an anonymous referee.

REFERENCES

Briegleb, B. P., C. M. Bitz, E. C. Hunke, W. H. Lipscomb, and J. L. Schramm, 2002: Description of the Community Climate System

Model Version 2 Sea Ice Model. NCAR Tech. Note, 62 pp. [Available online at http://www.ccsm.ucar.edu/models.]
Carissimo, B. C., A. H. Oort, and T. H. Vonder Haar, 1985: Estimating the meridional energy transports in the atmosphere and ocean. *J. Phys. Oceanogr.,* **15,** 82–91.
Clement, A., and R. Seager, 1999: Climate and the tropical oceans. *J. Climate,* **12,** 3383–3401.
Curry, J. A, J. L. Schramm, D. K. Perovich, and J. O. Pinto, 2001: Applications of SHEBA/FIRE data to evaluation of snow/ice albedo parameterizations. *J. Geophys. Res.,* **106** (D14), 15 345–15 355.
Delworth, T. L, R. J. Stouffer, K. W. Dixon, M. J. Spelman, T. R. Knutson, A. J. Broccoli, P. J. Kushner, and R. T. Wetherald, 2002: Review of simulations of climate variability and change with the GFDL R30 coupled climate model. *Climate Dyn.,* **19,** 555–574.
Eicken, H., M. A. Lange, H.-W. Hubberten, and P. Wadhams, 1994: Characteristics and distribution patterns of snow and meteoric ice in the Weddel Sea and their contribution to the mass balance of sea ice. *Ann. Geophys.* **12,** 80–93.
GFDL GAMDT, 2003: The Geophysical Fluid Dynamics Laboratory (GFDL) new global atmosphere and land model AM2/LM2: Evaluation with prescribed SST simulations. *J. Climate,* submitted.
Gleckler, P. J., and Coauthors, 1995: Cloud-radiative effects on implied oceanic energy transports as simulated by atmospheric general circulation models. *Geophys. Res. Lett.* **22,** 791–794.
Gnanadesikan, A., 1999: A simple predictive model for the structure of the oceanic pycnocline. *Science,* **283,** 2077–2079.
Gregory, J. M., and J. F. B. Mitchell, 1997: The climate response to CO_2 of the Hadley Centre coupled AOGCM with and without flux adjustment. *Geophys. Res. Lett.,* **24,** 1943–1946.
Hartmann, D. L., M. E. Ockert-Bell, and M. L. Michelson, 1992: The effect of cloud type on Earth's energy balance: Global analysis. *J. Climate,* **5,** 1281–1304.
Held, I., 1999: The macroturbulence of the troposphere. *Tellus,* **51A–B,** 59–70.
——, 2001: The partitioning of the poleward energy transport between the tropical ocean and atmosphere. *J. Atmos. Sci.,* **58,** 943–948.
Hunke, E. C., and J. K. Dukowicz, 1997: An elastic–viscous–plastic model for sea ice dynamics. *J. Phys. Oceanogr.,* **27,** 1849–1867.
Jakob, C., and S. A. Klein, 2000: A parameterization of the effects of cloud and precipitation overlap for use in general circulation models. *Quart. J. Roy. Meteor. Soc.,* **126,** 2525–2544.
Klein, S. A., and D. L. Hartmann, 1993: The seasonal cycle of low stratiform cloudiness. *J. Climate,* **6,** 1587–1606.
Manabe, S., and R. J. Stouffer, 1997: Coupled ocean–atmosphere response to freshwater input: Comparison to Younger Dryas event. *Paleoceanography,* **12,** 321–336.
Martinson, D. G., and R. A. Iannuzzi, 1998: Antarctic ocean–ice interactions: Implications from ocean bulk property distributions in the Weddell gyre. *Antarctic Sea Ice: Physical Processes, Interactions and Variability,* M. D. Jeffries, Ed., Antarctic Research Series, Vol. 74, Amer. Geophys. Union, 243–271.
Milly, P. C. D., and A. B. Shmakin, 2002: Global modeling of land water and energy balances. Part I: The land dynamics (LaD) model. *J. Hydrometeor.* **3,** 283–299.
Moorthi, S., and M. J. Suarez, 1992: Relaxed Arakawa–Schubert: A parameterization of moist convection for general circulation models. *Mon. Wea. Rev.,* **120,** 978–1002.
Poulsen, C. J., R. T. Pierrehumbert, and R. L. Jacob, 2001: Impact of ocean dynamics on the simulation of the Neoproterozoic ''snowball Earth.'' *Geophys. Res. Lett.,* **28,** 1575–1578.
Rind, D., and M. Chandler, 1991: Increased ocean heat transports and warmer climate. *J. Geophys. Res.,* **96** (D4), 7437–7461.
Rotstayn, L. D., 1997: A physically based scheme for the treatment of stratiform clouds and precipitation in large-scale models. I: Description and evaluation of microphysical processes. *Quart. J. Roy. Meteor. Soc.,* **123,** 1227–1282.
——, B. Ryan, and J. Katzfey, 2000: A scheme for calculation of the liquid fraction in mixed-phase clouds in large-scale models. *Mon. Wea. Rev.,* **128,** 1070–1088.
Russell, G. L., J. R. Miller, and L.-C. Tsang, 1985: Seasonal oceanic heat transports computed from an atmospheric model. *Dyn. Atmos. Oceans,* **9,** 253–271.
Seager, R., D. S. Battisti, J. Yin, N. Gordon, N. Naik, A. C. Clement, and M. A. Cane, 2001: Is the Gulf Stream responsible for Europe's mild winters? *Quart. J. Roy. Meteor. Soc.,* **127,** 1–23.
Semtner, A. J., 1976: A model for the thermodynamics growth of sea ice in numerical investigations of climate. *J. Phys. Oceanogr.,* **6,** 379–389.
Sutton, R., and P.-P. Mathieu, 2002: Response of the atmosphere–ocean mixed-layer system to anomalous ocean heat-flux convergence. *Quart. J. Roy. Meteor. Soc.,* **128,** 1259–1275.
Tiedtke, M., 1993: Representation of clouds in large-scale models. *Mon. Wea. Rev.,* **121,** 3040–3061.
Toggweiler, J. R., and B. Samuels, 1995: Effect of Drake Passage on global thermohaline circulation. *Deep-Sea Res.,* **42A,** 477–500.
Trenberth, K. E., and J. M. Caron, 2001: Estimates of meridional atmosphere and ocean heat transports. *J. Climate,* **14,** 3433–3443.
Vellinga, M., and R. Wood, 2002: Global climate impacts of a collapse of the Atlantic thermohaline circulation. *Climate Change,* **54,** 251–267.
Winton, M., 1997: The effect of cold climate upon North Atlantic deep water formation in a simple ocean–atmosphere model. *J. Climate,* **10,** 37–51
——, 2000: A reformulated three-layer sea ice model. *J. Atmos. Oceanic. Technol.,* **17,** 525–531.